JPEDAV (2008) 29:312–321
DOI: 10.1007/s11669-008-9341-9
1547-7037 ©ASM International

Computational Study of Atomic Mobility in Co-Fe-Ni Ternary Fcc Alloys

Y. W. Cui, M. Jiang, I. Ohnuma, K. Oikawa, R. Kainuma, and K. Ishida

(Submitted April 27, 2007; in revised form January 31, 2008)

The generalized Boltzmann-Matano method has been used to evaluate the interdiffusion coefficients at 1100 °C for the fcc phase of the Co-Fe-Ni ternary system from the concentration profiles developed from single-phase diffusion couple. The evaluated interdiffusion coefficients, together with other experimental data in the literature, have been assessed to develop an atomic mobility database for the fcc phase of the Co-Fe-Ni ternary. The atomic mobility database, in conjunction with the CALPHAD-base thermodynamics, has been used to simulate a number of ternary diffusion couple experiments. Comprehensive comparisons between the calculated and experimental data show that excellent agreement is obtained not only for the general diffusion data of ternary diffusion couple, such as the interdiffusion coefficients and the concentration profiles, but also for much of in-depth diffusion behavior, like the diffusion path, the interdiffusion flux and the shift of the Kirkendall plane.

Keywords Boltzmann-Matano analysis, critical assessment, DICTRA modeling, diffusion, Kirkendall effect, ternary system

1. Introduction

Nowadays conventional Co-based high-temperature alloys are not as widely used as Ni-based and Ni-Fe-based alloys in high-temperature applications. This is mainly due to a fact that no intermetallic compound is suitable for strengthening at high temperature for the Co-based alloys, unlike the ordered face-centered cubic (fcc) phase γ' precipitated in the fcc matrix γ for the Ni-based superalloys. However, Co is often used as alloying element in many Ni-based high-temperature alloys.[1] Very recently, Co-based alloys with the presence of the $\gamma' + \gamma$ microstructure were found to offer promise as candidates for next-generation high temperature materials.[2] The morphology and composition of the γ' phase are dependent on the diffusion interaction between the γ' and γ phases. Diffusion process also governs much of heat treatment processing and performance of commercial Ni-based superalloys, and is expected to play the same role on the new type Co-based alloys. Knowledge of diffusion characteristics of the multicomponent Co-based systems is thus of critical importance not only in developing understanding of the commercial Ni-based superalloys, but also in exploring the engineering use of this new type of Co-based alloys. Over the years, the diffusion simulation based on the atomic mobility made important progresses such that it permits prediction of almost all aspects of diffusion-controlled phenomena, such as diffusion coefficients, concentration profiles, microstructural stability of the Kirkendall plane and lattice plane displacement.[3-6] By contrast, the atomic mobility databases are still very limited, so far, only available for the steel and Fe-alloys,[7,8] and the Ni-based alloys.[9] However, there is an increasing need for the atomic mobility imposed by advanced microstructural modeling for real materials,[10,11] as well as technological application. A project aiming at developing the atomic mobility database for the multicomponent Co-based alloys has been started up in the authors' group. So far, the atomic mobilities for some key elements and fundamental binary systems have been assessed.[12,13] It is then possible to extend the assessment for relevant critical Co-based ternaries, one of which is the Co-Fe-Ni system.

The Co-Fe-Ni system has complete solid solubility with the fcc structure at high temperature.[14] Due to this convenience, the interdiffusion coefficients of the Co-Fe-Ni system were measured at the temperatures 1136 and 1315 °C a long time ago.[15,16] Very recent works[17-20] turned interests on the determination of the average effective interdiffusion coefficients (D_{AEDC}) and the Kirkendall effect. Nevertheless, existing results are still not amenable to full understanding of diffusion behavior of the Co-Fe-Ni ternary system, especially the temperature and concentration dependences of diffusion coefficients. The D_{AEDC} achieves great success on the characterization of concentration profiles in single-phase multicomponent diffusion couples,[21,22] however, is hard to extract the atomic mobility information. Accordingly, the purpose of this work is to perform a comprehensive evaluation of the interdiffusion coefficients and assess the atomic mobility for the fcc phase

Y. W. Cui, M. Jiang, I. Ohnuma, K. Oikawa, and **K. Ishida,** Department of Materials Science, Graduate School of Engineering, Tohoku University, Sendai 980-8579, Japan; **Y. W. Cui, K. Oikawa, R. Kainuma,** and **K. Ishida,** Core Research for Evolutional Science and Technology (CREST), Japan Science and Technology Agency (JST), Kawaguchi, Saitama 332-0012, Japan; **R. Kainuma,** Institute of Multidisciplinary Research for Advanced Materials (IMRAM), Tohoku University, Sendai 980-8577, Japan. Contact e-mail: ycui2005@gmail.com

of the Co-Fe-Ni ternary, and finally provide insights into its diffusion characteristics by performing simulations of interdiffusion behaviors with the assessed atomic mobilities.

2. Interdiffusion Coefficient and Modeling

2.1 Evaluation of Interdiffusion Coefficient

The interdiffusion and the Kirkendall effect at 1100 °C have been very recently studied by Ugaste et al.[17,18] However, only the D_{AEDC} has been determined from the concentration profiles developed during the isothermal diffusion. The tabulated concentration profiles provided by Ugaste et al.[17] allow an evaluation of the interdiffusion coefficients at 1100 °C by using the generalized Boltzmann-Matano analysis due to Kirkaldy,[23] which requires a pair of diffusion couples with intersecting diffusion path to determine the interdiffusion coefficient at the intersecting composition.[23,24] The starting equation for the analysis of the Co-Fe-Ni ternary alloys is Fick's first law for the interdiffusion fluxes of Co and Ni with Fe as dependent species, when the partial molar volume of each species is assumed to be constant, it is written by

$$\tilde{J}_i = \frac{1}{2t}\int_{x_i^+ \text{ or } x_i^-}^{x_i(z)} (z - z_0)\mathrm{d}x_i = -\sum_j \tilde{D}_{ij}^{\mathrm{Fe}} \frac{\partial x_j}{\partial z} \quad (i,j = \mathrm{Co}, \mathrm{Ni}), \tag{Eq 1}$$

where x_i is the atomic fraction of species i, x_i^+ and x_i^- are the atomic fractions for i at either end of the diffusion couple, z is the distance, z_0 is the Matano plane for the diffusion couple, t is the diffusion time, and $\tilde{D}_{ij}^{\mathrm{Fe}}$ is the interdiffusion coefficient with Fe as dependent species. The interdiffusion fluxes and concentration gradients are evaluated at the common composition for the individual components from their concentration profiles for the pairs. Upon Eq 1, four independent relations can be set up and solved for four interdiffusion coefficients at the common composition.

In this work, the experimental concentration profiles measured by Ugaste et al.[17] were firstly smoothed by using the Piecewise Cubic Hermite Interpolating Polynomial (PCHIP).[25] The interdiffusion flux is the numerically evaluated integral that was obtained by using the adaptive Simpson Quadrature (ASQ) from the smoothed concentration profiles. The concentration gradient was computed by evaluating the derivative of the interpolating polynomial from the coefficients of the PCHIP polynomial,[26] thus lowering the subjective steps which are the main sources of errors encountered in some diffusivity measurements.[27]

2.2 Atomic Mobility and Diffusivity

Andersson and Agren[3] suggested that the atomic mobility M_i of species i could be expressed as a function of temperature T,

$$M_i = M_i^0 \exp\left(\frac{-Q_i^S}{RT}\right)\frac{1}{RT}, \tag{Eq 2}$$

where Q_i^S is the activation energy, M_i^0 is the frequency factor and R is the gas constant. Note that the mobility parameters in the DICTRA notation (DIffusion Controlled TRAnsformation),[8] $-Q_i^S$ and $RT \ln M_i^0$, can be grouped into one single parameter, $Q_i = -Q_i^S + RT \ln M_i^0$, in case when there is no magnetic effect on the atomic mobility. The parameter Q_i is assumed to be of the composition dependence,[4] and can be expressed by the Redlich-Kister polynomial in composition,

$$Q_i = \sum_p x_p Q_i^p + \sum_p \sum_{q>p} x_p x_q \left[\sum_{r=0,1,2,\ldots} {}^{r}Q_i^{p,q}(x_p - x_q)^r\right] + \sum_p \sum_{q>p} \sum_{v>q} x_p x_q x_v [v_{pqv}^s \, {}^{s}Q_i^{p,q,v}], \quad (s = p,q,v), \tag{Eq 3}$$

where x_p is the mole fraction of species p, Q_i^p is the value Q_i of species i in pure species p, ${}^{r}Q_i^{p,q}$ and ${}^{s}Q_i^{p,q,v}$ are the binary and ternary interaction parameters, and the parameter v_{pqv}^s is given by $v_{pqv}^s = x_s + (1 - x_p - x_q - x_v)/3$. The tracer diffusion coefficient D_i^* is rigorously related to the atomic mobility by a simple relation, $D_i^* = RTM_i$. The interdiffusion coefficient with n as dependent species, $\tilde{D}_{pq}^n$, can be derived by,

$$\tilde{D}_{pq}^n = \sum_i (\delta_{ip} - x_p) x_i M_i \left(\frac{\partial \mu_i}{\partial x_q} - \frac{\partial \mu_i}{\partial x_n}\right), \tag{Eq 4}$$

where the Kronecker delta $\delta_{ip} = 1$ when $i = p$ and 0 otherwise, and μ_i is the chemical potential of species i. Note that the superfix 'n' means the dependent species throughout the paper. The chemical mobility matrix (defined in the laboratory reference frame) can be written as function of the atomic mobility M_i,[3,28]

$$\tilde{M}_{ii}^n = \frac{1}{V_m}\{(1 - x_i)x_i M_i - x_i[(1 - x_i)x_i(M_i - M_n) - x_i x_j(M_j - M_n)]\}; \tag{Eq 5a}$$

$$\tilde{M}_{ij}^n = \frac{1}{V_m}\{-x_i x_j M_j - x_j[(1 - x_i)x_i(M_i - M_n) - x_i x_j(M_j - M_n)]\}, \quad (i,j = \mathrm{Co}, \mathrm{Ni},\ i \neq j,\ n = \mathrm{Fe}) \tag{Eq 5b}$$

where V_m is the molar volume. Upon the proposed relations, the atomic mobility parameter Q_i can be numerically assessed by fitting to reliable experimental diffusion coefficients.

2.3 Shift of the Kirkendall Marker and Displacement of Lattice Plane

In a diffusion couple where the partial molar volume of each species is assumed to be constant, the rate of change of composition in the diffusion zone can be described by the continuity equation, for a Co-Fe-Ni ternary couple, i.e.

$$\frac{1}{V_m}\frac{\partial x_i}{\partial t} = \sum_{k=\mathrm{Co,Ni}} \nabla \cdot \tilde{M}^n_{ik} \nabla[\mu_k - \mu_n], \quad (n = \mathrm{Fe}). \qquad \text{(Eq 6)}$$

Equation 6 can be solved numerically corresponding to different initial conditions and boundary conditions. The solution expresses the form of the concentration profile. If diffusion occurs by a vacancy mechanism, the nonuniform velocity of the inert markers with respect to the laboratory-fixed frame of reference is dependent on the difference of the intrinsic diffusivities D^n_{ik} of the species and the concentration gradients,[6]

$$\frac{v}{V_m} = J_{Va} = \left(-\sum_{i=\mathrm{Co,Fe,Ni}} J_i\right) \qquad \text{(Eq 7a)}$$

$$J_i = -\frac{1}{V_m}\sum_{k=\mathrm{Co,Ni}} D^n_{ik}\frac{\partial x_i}{\partial z}, \quad (n = \mathrm{Fe}), \qquad \text{(Eq 7b)}$$

where J_i is the flux of species i relative to the lattice-fixed frame of reference. In a diffusion controlled interaction, the Kirkendall plane is the only plane that stays at a constant composition during the whole diffusion annealing and moves parabolically in time with a velocity, i.e.

$$v_k = \frac{dz}{dt} = \frac{z_k - z_{k0}}{2t} = \frac{z_k}{2t}, \qquad \text{(Eq 8)}$$

where z_k and z_{k0} (=0) are the positions of the Kirkendall plane at times $t = t$ and $t = 0$, respectively. As a result, the Kirkendall plane can be graphically determined from the Kirkendall velocity construction,[29,30] i.e. a plot of the velocity of the inert markers as a function of the distance, by finding the intersection between the marker velocity curve determined by Eq 7(a) and the straight line by Eq 8.

3. Results and Discussion

3.1 Interdiffusion Coefficient at 1100 °C

Prior to evaluation of the interdiffusion flux and the concentration gradient, the experimental concentration profiles[17] were smoothed by the PCHIP interpolation. An example as applied to the diffusion couple C1 (Co/Co-37at.% Fe-45at.% Ni) is presented in Fig. 1(a). Figure 1(b) shows the interdiffusion flux integrated by using the ASQ. The existence of a zero flux plane (ZFP) for Ni has been identified in Fig. 1(b), at which location the interdiffusion flux of Ni changes direction. The ZFPs were also examined for all other couples fabricated by Ugaste et al.,[17] and only the couple C3 (Ni/Co-40at.% Fe) was found to exhibit a ZFP for Co. Meantime, four diffusion couples, C1, C3, C4 (Co-49at.% Ni/Co-41at.% Fe), and C7 (Co-77at.% Fe/Co-70at.% Ni), exhibit extremes (maximum or minimum or both) in their concentration profiles, which are also termed as "Darken-type" couple.[24] If it is a Darken-type couple, the two concentration profiles from a single diffusion couple lead to determination of one main

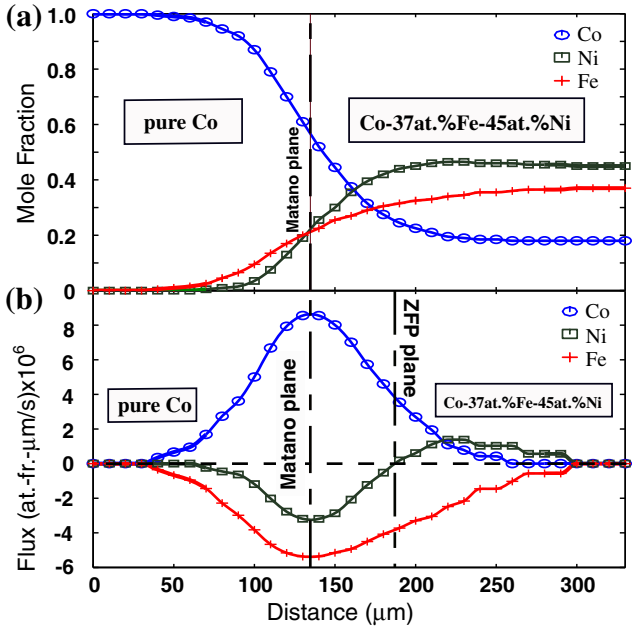

Fig. 1 (a) Smoothed concentration profiles for ternary diffusion couple C1 (Co/Co-37at.% Fe-45at.% Ni) after annealing at 1110 °C for 196 h by the using the Piecewise Cubic Hermite Interpolating Polynomial; (b) Computed interdiffusion flux by using the adaptive Simpson Quadrature. Symbols are from the experimental measurement[17]

and one cross-interdiffusion coefficients at the composition of the extreme. The evaluated interdiffusion coefficients at 1100 °C are summarized in Table 1 and are also plotted in Fig. 2. All evaluated interdiffusion coefficients in this work were examined according to the thermodynamic constraints for ternary diffusion coefficients,[31]

$$\tilde{D}^{\mathrm{Fe}}_{\mathrm{CoCo}} + \tilde{D}^{\mathrm{Fe}}_{\mathrm{NiNi}} > 0 \qquad \text{(Eq 9a)}$$

$$\left(\tilde{D}^{\mathrm{Fe}}_{\mathrm{CoCo}} \times \tilde{D}^{\mathrm{Fe}}_{\mathrm{NiNi}}\right) - \left(\tilde{D}^{\mathrm{Fe}}_{\mathrm{CoNi}} \times \tilde{D}^{\mathrm{Fe}}_{\mathrm{NiCo}}\right) \geq 0 \qquad \text{(Eq 9b)}$$

$$\left(\tilde{D}^{\mathrm{Fe}}_{\mathrm{CoCo}} + \tilde{D}^{\mathrm{Fe}}_{\mathrm{NiNi}}\right)^2 \geq 4\left(\tilde{D}^{\mathrm{Fe}}_{\mathrm{CoCo}} \times \tilde{D}^{\mathrm{Fe}}_{\mathrm{NiNi}} - \tilde{D}^{\mathrm{Fe}}_{\mathrm{CoNi}} \times \tilde{D}^{\mathrm{Fe}}_{\mathrm{NiCo}}\right) \qquad \text{(Eq 9c)}$$

Questionable coefficients that violate the constraints were removed from Table 1 and Fig. 2. Other suspicious coefficients are those determined from the couple C3, as well as C2 (Fe/Co-49at.% Ni), C4, C5 (Co-30at.% Ni/Co-60at.% Fe), which have been identified to be remarkably greater than the diffusivities of close compositions. As pointed out by Okamoto and Massalski,[32] though the phase rules are not violated, an abrupt change of thermodynamic property of phase, as one contribution to the diffusivity, is thermodynamically improbable if without being accompanied by a first-order phase transformation. It is a reasonable approximation to assume that the atomic mobility, another contribution to the diffusivity, obey a

Table 1 Interdiffusion coefficients ($D \times 10^{15}$ m^2/s) at 1100 °C extracted from the diffusion couple experiments of Ugaste et al.[17]

Diffusion couples	Co, at.%	Ni, at.%	$\tilde{D}^{Fe}_{CoCo}$	$\tilde{D}^{Fe}_{CoNi}$	$\tilde{D}^{Fe}_{NiCo}$	$\tilde{D}^{Fe}_{NiNi}$
C1-C2	36.3	36.3	2.9	2.6	2.0	3.4
C1-C4	55.0	23.3	1.9	1.2	1.4	2.5
C1-C5	57.5	21.5	2.3	1.9	0.8	1.7
C1-C6	23.9	44.3	2.3	1.2	2.5	3.9
C2-C3	39.1	38.5	3.8 (a)	1.3 (a)	0.5 (a)	4.9 (a)
C2-C7	27.5	27.9	3.4	1.5	2.4	2.6
C4-C5	56.2	20.2	2.7	1.6	0.2 (a)	1.9
C3 local maximum of Co	61.5	3.2		1.2		2.3 (a)
C4 local maximum of Co	62.5	4.2		1.8		1.9 (a)
C4 local minimum of Co	48.0	42.0		1.0		2.3
C7 local maximum of Co	30.5	10.2		0.81		0.94
C7 local minimum of Co	24.0	48.0		1.1		3.7

(a) denotes the marked data probably in large uncertainty and not used in the optimization process

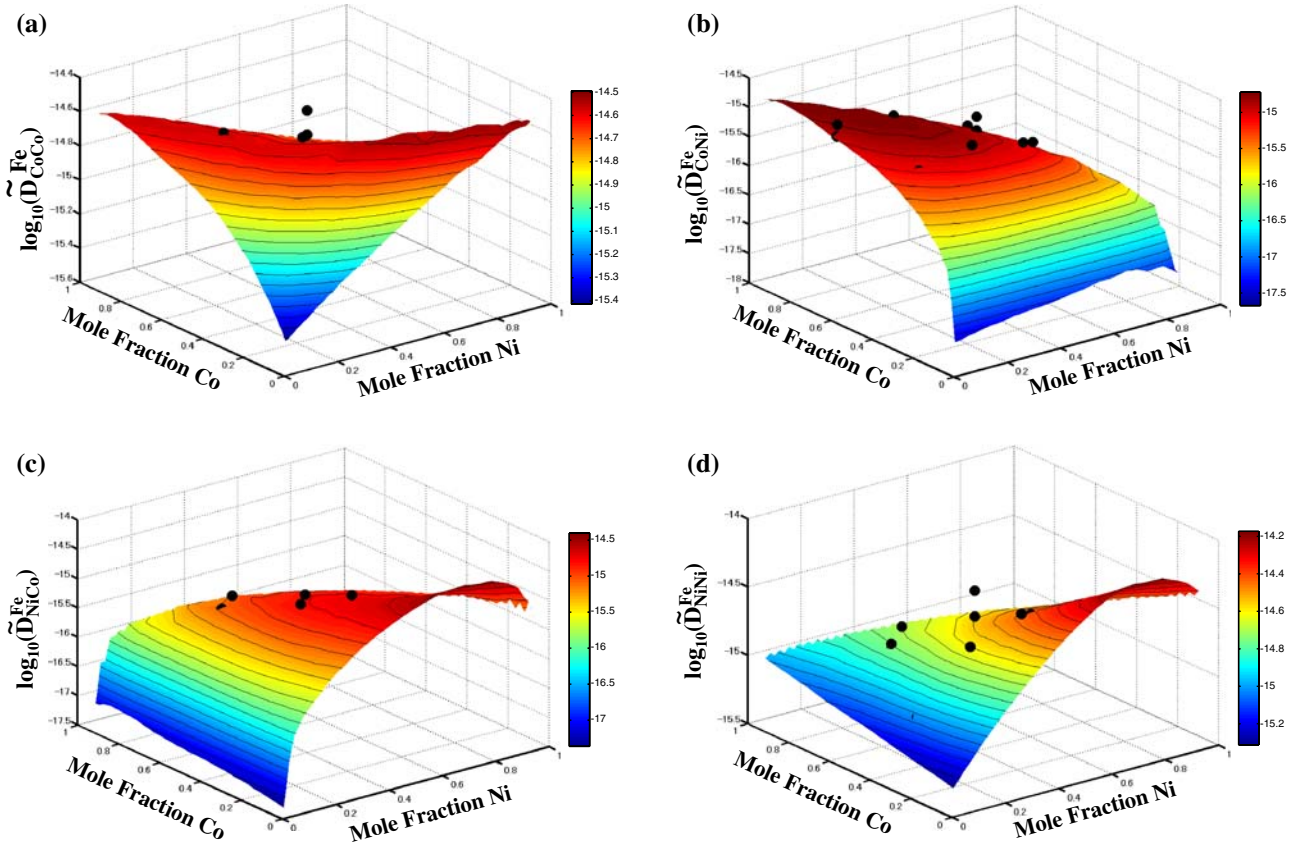

Fig. 2 Logarithm plot of the interdiffusion coefficients of ternary Co-Fe-Ni alloys at 1100 °C, (a) $\log_{10}\tilde{D}^{Fe}_{CoCo}$; (b) $\log_{10}\tilde{D}^{Fe}_{CoNi}$; (c) $\log_{10}\tilde{D}^{Fe}_{NiCo}$; (d) $\log_{10}\tilde{D}^{Fe}_{NiNi}$. Black lines are 3D contour lines. Symbols are the experimental values evaluated in this work

similar guide when neither a first-order phase transformation nor a change in diffusion mechanism of material takes place. As a result, the relevant data, footnoted in Table 1, were believed to have large uncertainty, and excluded from the assessment procedure of the atomic mobility.

3.2 Assessing Atomic Mobility

The interdiffusion coefficients evaluated in this work, together with those measured by Sabatier and Vignes,[15,16] have been optimized to obtain the ternary interactions of atomic mobility parameters for the Co-Fe-Ni ternary fcc alloys by using the DICTRA software.[33] The results of the assessment, together with the unary and binary parameters,[4,13,34] are listed in Table 2. In the sections that follow, focus will be placed on comparison between the calculated and experimental diffusion coefficients.

The calculated interdiffusion coefficients of the Co-Fe-Ni system with Fe as dependent species are presented as 3D surface plots in Fig. 2 for the temperature at 1100 °C and in Fig. 3 at 1315 °C, with the experimental data shown for comparison. Note that a colorbar was added to each 3D plot to specify the values of the interdiffusion coefficients. Excellent agreements were obtained between the calculated and experimental data in all the cases with the only exception of the suspicious data mentioned in Section 3.1. This also means that the evaluated interdiffusion coefficients in this work behave in good accord with the early experimental data.[15,16] The discrepancies with the measured coefficients are slightly greater for the cross coefficients of $\tilde{D}^{Fe}_{CoNi}$ and $\tilde{D}^{Fe}_{NiCo}$, see Fig. 2(b, c) and 3(b, c), in which cases the calculations differ at largest by a factor of 2 from the measurements. More details about the variation of interdiffusion coefficients in the concentration can be obtained from the surface plots, e.g., $\tilde{D}^{Fe}_{CoCo}$ strongly increases with increasing Co and Ni concentrations, while $\tilde{D}^{Fe}_{CoNi}$ increases solely with Co concentration; by contrast, both $\tilde{D}^{Fe}_{NiCo}$ and $\tilde{D}^{Fe}_{NiNi}$ increase with increasing Ni concentration and weakly depend on Co concentration. Note that Vignes and Sabatier[16] observed that $\tilde{D}^{Fe}_{NiNi}$ and $\tilde{D}^{Fe}_{NiCo}$ both present strong maxima approximately in the vicinity of the Fe-Ni boundary at 75 at.% Ni at 1315 °C. Such concentration dependence was confirmed not only for 1315 °C in Fig. 3(c, d), but also for 1100 °C in Fig. 2(c, d). That $\tilde{D}^{Fe}_{CoNi}$ is obviously less than $\tilde{D}^{Fe}_{CoCo}$ can be evident in these plots, thereby indicating the Co concentration gradient has a greater effect on the Co diffusion than does the Ni concentration gradient. Likewise, the Ni concentration gradient has a greater effect on the Ni diffusion than does the Co concentration gradient. The calculated chemical mobility of the Co-Fe-Ni system is shown in Fig. 4(a, c). The overall agreement between the calculated and measured chemical mobility is less good than that for the interdiffusion coefficients. This is due to a fact that the experimental chemical mobilities were in fact estimated from the measured interdiffusion coefficients by assuming the Co-Fe-Ni system to be thermodynamically ideal, as such, neither binary nor ternary interaction was taken into account in the thermodynamic sense.[16] Our chemical mobility parameters were assessed by fitting to the same set of interdiffusion data, however, the regular-solution interaction was used thermodynamically for all three binary systems.[14]

Another set of cross coefficients, defined with respect to Co as dependent species, is given in Fig. 5. It is apparent that the cross coefficient $\tilde{D}^{Co}_{FeNi}$ is quite small, namely, at least one order of magnitude smaller than the main coefficients (see Fig. 5a), and another cross coefficient $\tilde{D}^{Co}_{NiFe}$ is negative over the entire concentration range (see Fig. 5b), both in good accord with observation and theory.[16] Comparison of Fig. 5(b) and 3(c, d), also reveals that, though the shapes of contours of $\tilde{D}^{Fe}_{NiCo}$, $\tilde{D}^{Fe}_{NiNi}$, and $\tilde{D}^{Co}_{NiFe}$ are similar, the concentration variation for $\tilde{D}^{Co}_{NiFe}$ is actually opposite to the former two.

Table 2 Assessed atomic mobilities for the fcc phase of the Co-Fe-Ni ternary

Mobility	Parameter, J/mole	Reference
Mobility of Co		
Q^{Co}_{Co}	−301654 − 70.10 * T	[13]
Q^{Fe}_{Co}	−301900 − 76.58 * T	[34]
Q^{Ni}_{Co}	−284724 − 69.23 * T	[13]
$Q^{Co,Ni}_{Co}$	−5000	[13]
${}^{0}Q^{Co,Fe}_{Co}$	+305495 − 201.71 * T	[13]
${}^{0}Q^{Co,Fe,Ni}_{Co}$	−826550	This work
${}^{1}Q^{Co,Fe,Ni}_{Co}$	319460	This work
${}^{2}Q^{Co,Fe,Ni}_{Co}$	494820	This work
Mobility of Fe		
Q^{Co}_{Fe}	−253301 − 97.97 * T	[34]
Q^{Fe}_{Fe}	−286000 − 79.55 * T	[4]
Q^{Ni}_{Fe}	−287000 − 67.5 * T	[4]
${}^{0}Q^{Co,Fe}_{Fe}$	−63300 + 48.68 * T	[13]
${}^{0}Q^{Fe,Ni}_{Fe}$	−115000 + 104 * T	[4]
${}^{1}Q^{Fe,Ni}_{Fe}$	+78800 − 73.3 * T	[4]
${}^{0}Q^{Co,Fe,Ni}_{Fe}$	8688	This work
${}^{1}Q^{Co,Fe,Ni}_{Fe}$	514100	This work
${}^{2}Q^{Co,Fe,Ni}_{Fe}$	−265830	This work
Mobility of Ni		
Q^{Co}_{Ni}	−315816 − 57.16 * T	[13]
Q^{Fe}_{Ni}	−286000 − 86 * T	[4]
Q^{Ni}_{Ni}	−287000 − 69.80 * T	[4]
${}^{0}Q^{Co,Ni}_{Ni}$	+9335	[13]
${}^{0}Q^{Fe,Ni}_{Ni}$	+124000 − 51.4 * T	[4]
${}^{1}Q^{Fe,Ni}_{Ni}$	−300000 + 213 * T	[4]
${}^{0}Q^{Co,Fe,Ni}_{Ni}$	−185730	This work
${}^{1}Q^{Co,Fe,Ni}_{Ni}$	−6610	This work
${}^{2}Q^{Co,Fe,Ni}_{Ni}$	−38480	This work

4. Diffusion Simulations

An efficient test of the validity the assessed atomic mobility not only includes comparison with measured diffusion coefficients, but also ability to predict the concentration profiles, the diffusion path and other in-depth diffusion behavior resulting from interdiffusion. In conjunction with CALPHAD-base thermodynamics, solving Eqs. 6 and 7 numerically enables much of the diffusion phenomena of the ternary diffusion couples to be predicted.

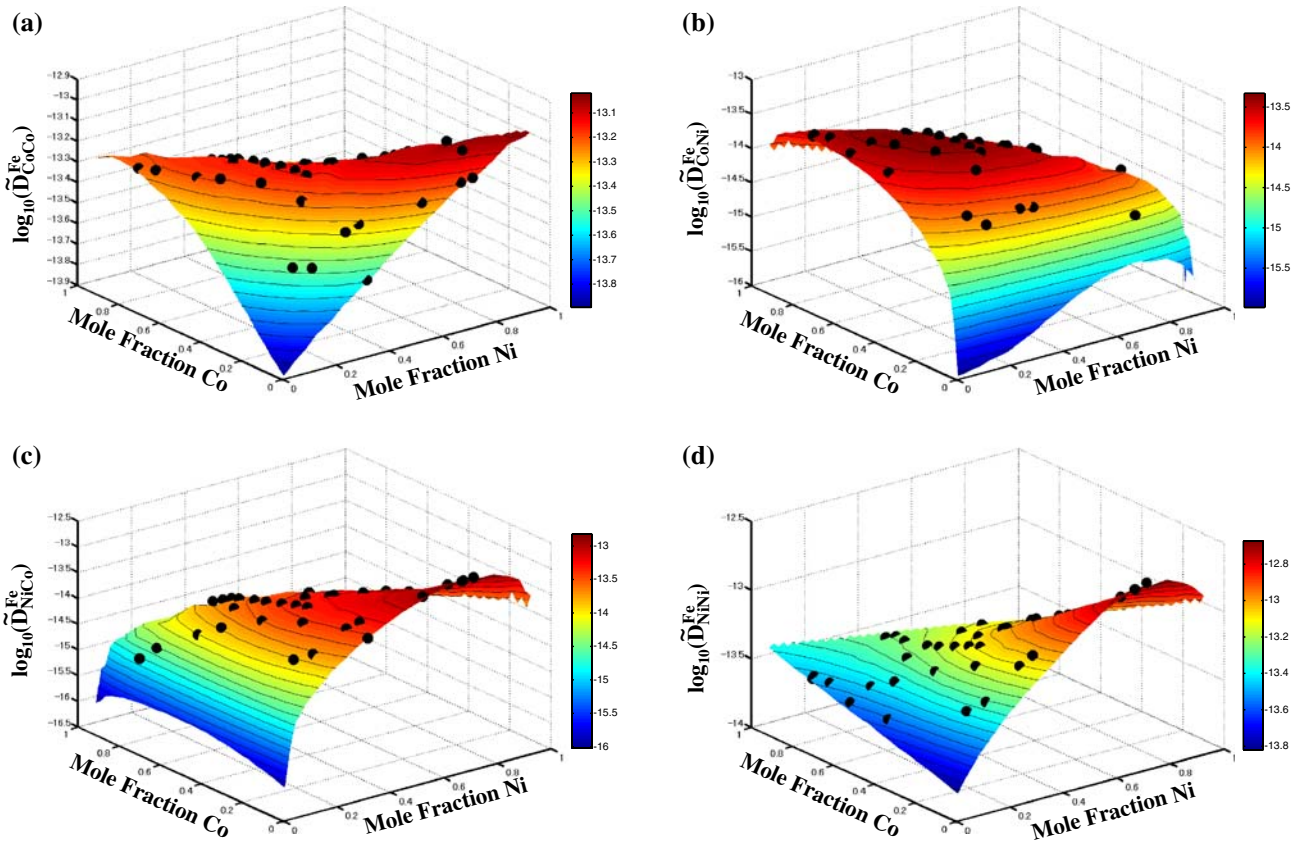

Fig. 3 Logarithm plot of the interdiffusion coefficients of ternary Co-Fe-Ni alloys at 1315 °C, (a) $\log_{10}\tilde{D}^{Fe}_{CoCo}$; (b) $\log_{10}\tilde{D}^{Fe}_{CoNi}$; (c) $\log_{10}\tilde{D}^{Fe}_{NiCo}$; (d) $\log_{10}\tilde{D}^{Fe}_{NiNi}$. Black lines are 3D contour lines. Symbols are from the experimental measurements[16]

4.1 Concentration Profiles and Diffusion Path of Ternary Diffusion Couples

The diffusion simulation has been set up to model a number of semi-infinite ternary diffusion-couple experiments, which were conducted under different initial conditions and heat treatment processes in the literature.[16,17,20] The current simulations were compared with the experimental concentration profiles not used in the optimization process. Very good agreement is obtained between our simulations and the experimental measurements for almost all diffusion-couples.[16,17,20] Representative concentration profiles calculated for the couples are shown in Fig. 6(a-c), superimposed also the experimental data. Note that the departure from the initial constants of Ni concentration, as a measure of the cross diffusion coefficients, was well reproduced in Fig. 6(b, c). The good agreement between the simulated concentration profiles and experimental measurements reflects a good mapping of the interdiffusion coefficients of the present assessment. However, two exceptions were raised for the couples C1 (see Fig. 6d) and C3, in which there are systematic discrepancies of several atomic percents between the calculated and measured concentration profiles.[17] Close inspection suggests that the causes of discrepancies are different for the two couples. The deviation for the couple C1 results from the fact that the impurity diffusivity of Fe in the pure fcc Co was fixed according to the radioactive tracer diffusion experiment.[13,34] Whereas for the couple C3, it is simply because most of interdiffusion coefficients evaluated from the C3 were identified by Eq 9(c) with wrong signs of the cross coefficients and for that reason eliminated from this work. All the simulated concentration profiles for the ternary couples at 1100 °C were further plotted in Fig. 7 as the diffusion path. The simulations are in good agreement with the experimental measurements.[17]

4.2 Interdiffusion Flux and Kirkendall Velocity Construction

Comparison can be also made for some in-depth diffusion behavior. The evaluation of the interdiffusion flux in Section 3.1 allows for the first time to compare the predicted fluxes with the experimental values. Figure 8 shows the simulated interdiffusion flux obtaining excellent agreement with the evaluated values for the couple C7. Figure 9(a) illustrates the Kirkendall velocity construction for the couple C6 (Co-51at.% Ni/Co-40at.% Fe-40at.% Ni) annealing at 1100 °C.[17] Note that the reduced velocity

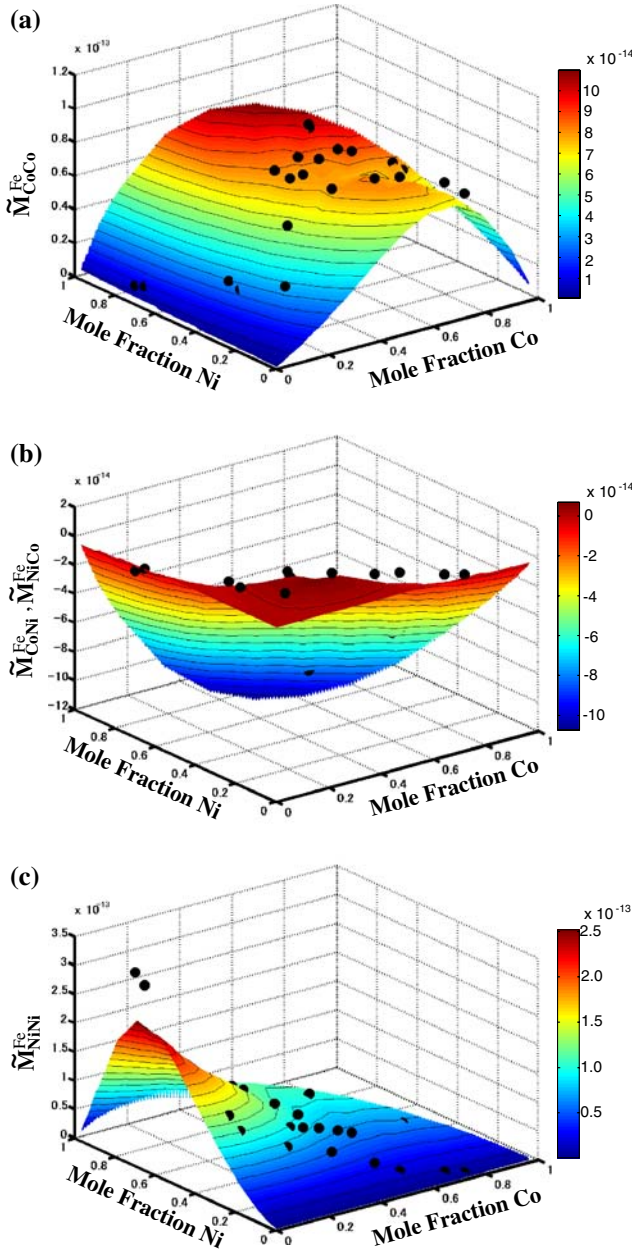

Fig. 4 Chemical mobilities of ternary Co-Fe-Ni alloys at 1315 °C, (a) $\tilde{M}^{Fe}_{CoCo}$; (b) $\tilde{M}^{Fe}_{CoNi}$ and $\tilde{M}^{Fe}_{NiCo}$; (c) $\tilde{M}^{Fe}_{NiNi}$. Black lines are 3D contour lines. Symbols are from the experimental measurements[16]

curve $v\sqrt{t}$ intersects the straight line $vt = z/2\sqrt{t}$ (determined by Eq 8) at a point with a negative gradient. As a result, there is a stable Kirkendall plane for the couple C6, i.e. the Kirkendall marker remains sharply concentrated.[29] Conversely, the couple C7 exhibits an intersection with a positive gradient, and thus an unstable Kirkendall plane occurs for the couple C7, i.e. the Kirkendall plane is dispersed. Therefore, the Kirkendall plane appearance inside a Co-Fe-Ni ternary couple, i.e. stable or unstable, may vary with the initial compositions of the end-members of the

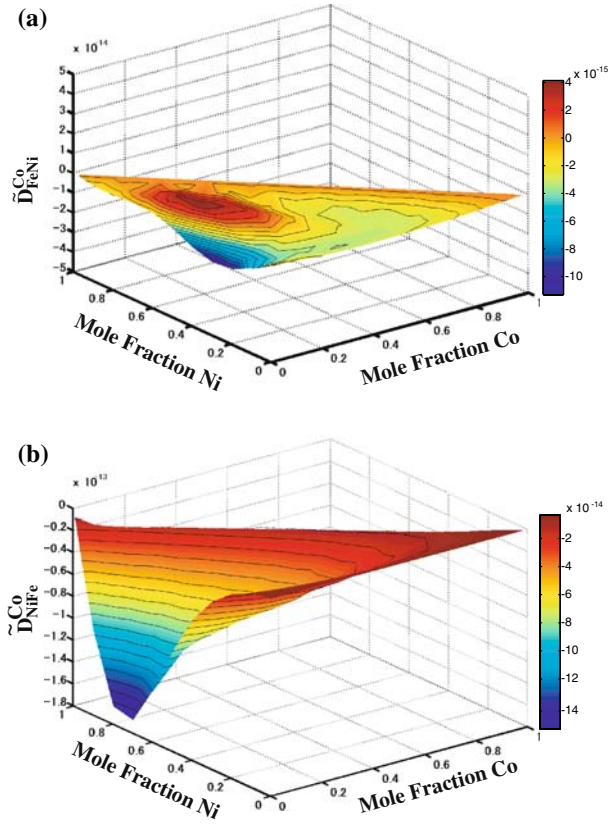

Fig. 5 Interdiffusion coefficients of ternary Co-Fe-Ni alloys at 1100 °C. Black lines are 3D contour lines. (a) $\tilde{D}^{Co}_{FeNi}$; (b) $\tilde{D}^{Co}_{NiFe}$

diffusion couple. The predicted shifts of the Kirkendall plane for the ternary couples C6 and C7 are 7.6 and 17.8 μm, which compare favorably with the experimental values, 8 and 19 μm, respectively.[17] Reasonable agreements, generally within 2-3 μm, were also obtained for the other couples fabricated by Ugaste et al.,[17] however, once again with exceptions of C1 and C3 due to the same reasons addressed before.

5. Conclusions

(i) The interdiffusion coefficients at 1100 °C for the fcc phase of the Co-Fe-Ni ternary system have been evaluated from the concentration profiles for single-phase diffusion couples by using the generalized Boltzmann-Matano method. The evaluated interdiffusion coefficients were found to behave in good accord with the earlier experimental data.

(ii) The evaluated interdiffusion coefficients, together with the previous data in the literature, have been assessed to develop an atomic mobility database for the Co-Fe-Ni ternary system. Good agreement was obtained between the calculated interdiffusion coefficients and the experimental values.

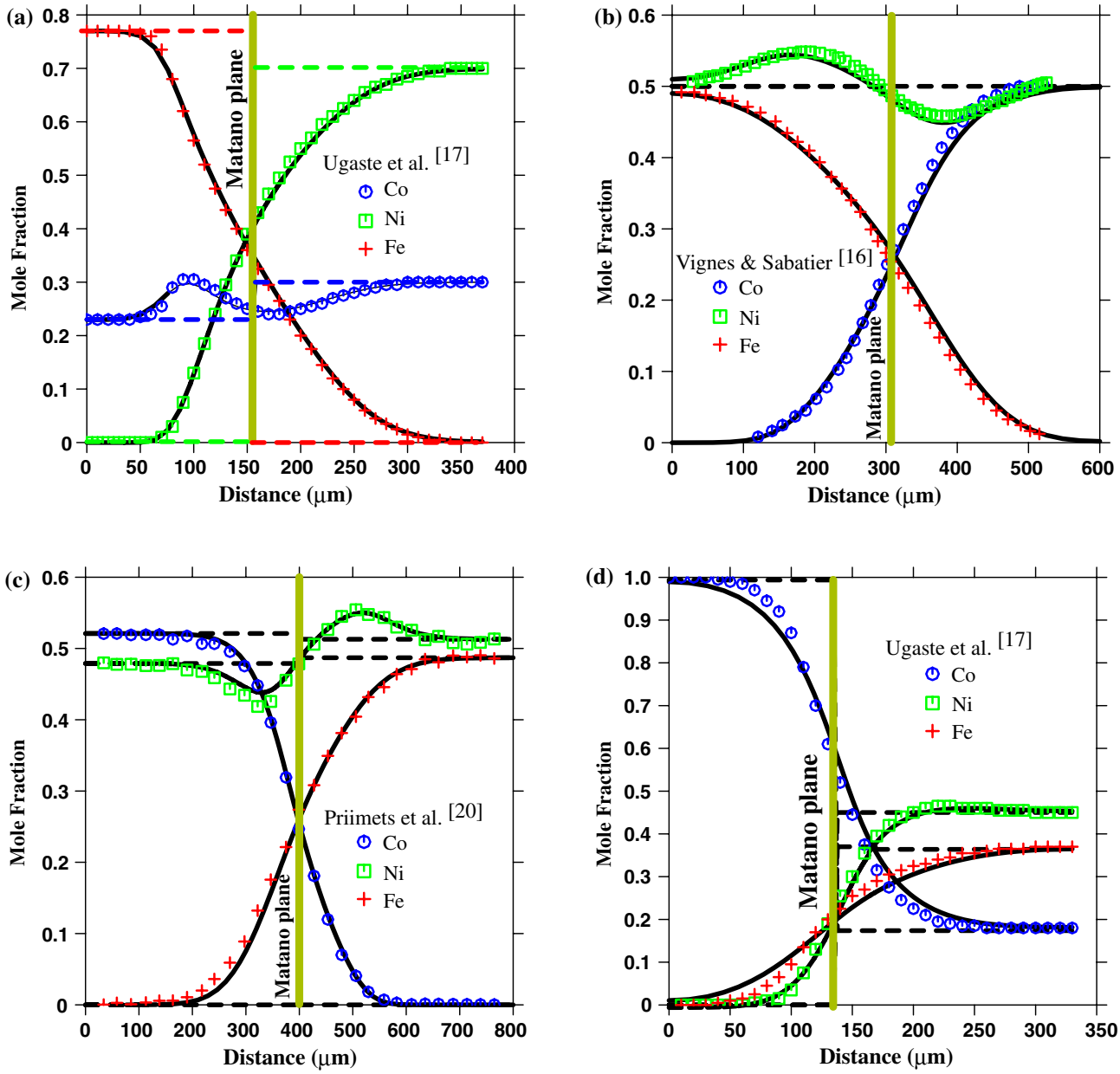

Fig. 6 Calculated concentration profiles for ternary diffusion couples, (a) C7 (Co-77at.% Fe/Co-70at% Ni) at 1100 °C for 196 h; (b) V8 (Fe-50at.% Ni/Co-50at.% Ni) at 1315 °C for 17 h; and (c) P5 (Co-47.9at.% Ni/Fe-51.3at.% Ni) at 1200 °C for 59 h; (d) C1 (Co/Co-37at.% Fe- 45at% Ni) at 1100 °C for 196 h. Symbols are from the experimental measurements[16,17,20]

(iii) The assessed atomic mobilities, in conjunction with the CALPHAD-type thermodynamic description, have been successfully used to predict many Co-Fe-Ni ternary-couple experiments. Comprehensive comparisons made between the predicted and experimental data show that excellent agreement was obtained not only for the concentration profiles and the diffusion path, but also for other in-depth diffusion behaviors, like the shift of the Kirkendall plane and the interdiffusion flux, even though no such experimental data were directly used in the optimization process of the atomic mobility.

Acknowledgments

This work was supported by CREST, Japan Science and Technology Agency. YC gratefully acknowledges to the 21st century COE program for financial support.

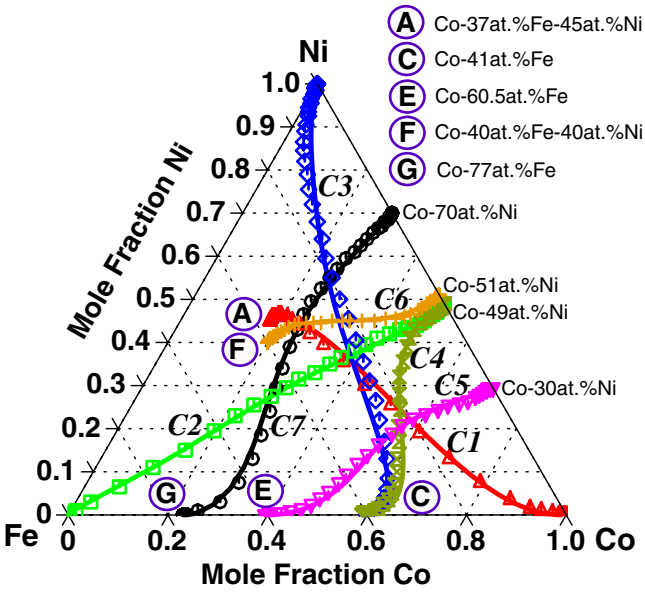

Fig. 7 Calculated diffusion path for the ternary diffusion couples after annealing at 1100 °C for 196 h. Symbols are from the experimental measurements[17]

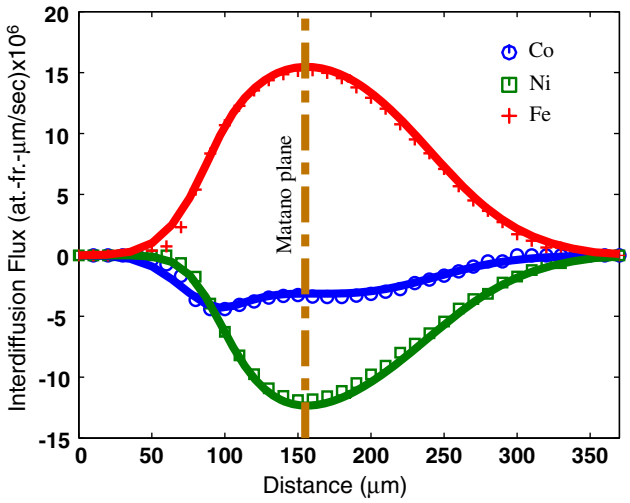

Fig. 8 Calculated interdiffusion flux for ternary diffusion couple C7 (Co-77at.%Fe/Co-70at.%Ni) at 1100 °C for 196 h. Symbols are the experimental points evaluated in the present work

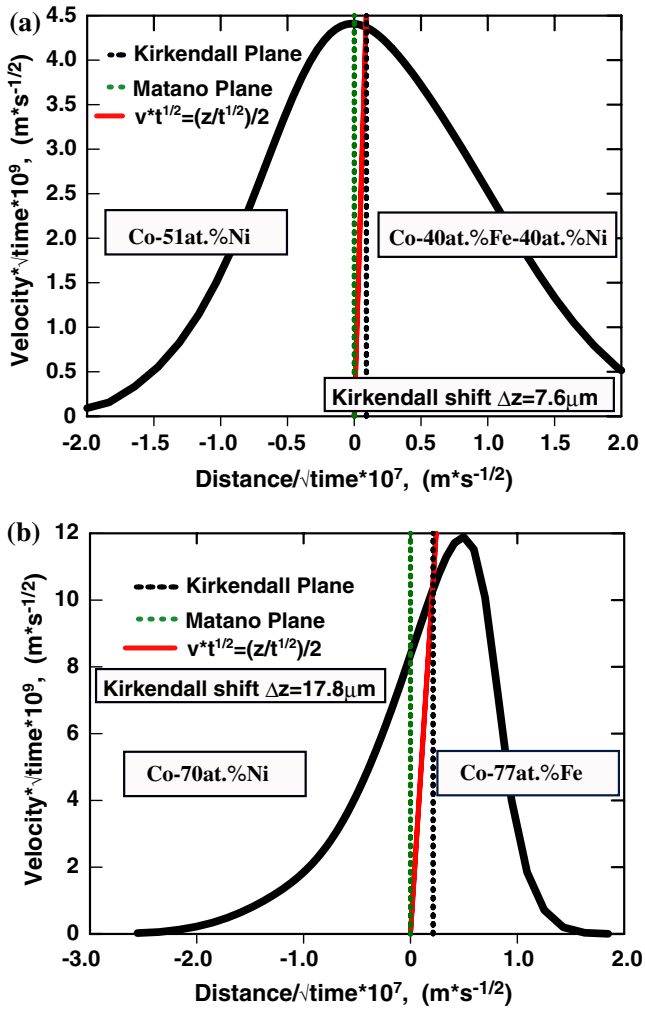

Fig. 9 Kirkendall velocity construction of the diffusion couples after annealing at 1100 °C for 196 h. Note that the Fe-rich end-member is placed on the right side of plot to give a better view. (a) C6 (Co-51at.%Ni/Co-40at.%Ni-40at.%Fe); (b) C7 (Co-70at.%Ni/Co-77at.%Fe)

References

1. S. Walston, A. Cetel, R. MacKay, K. O'Hara, D. Duhl, and R. Dreshfield, Joint Development of a Fourth Generation Single Crystal Superalloy, *Superalloys 2004*, K.A. Green, T.M. Pollock, H. Harada, T.E. Howson, R.C. Reed, J.J. Schirra, and S. Walston, Eds., Warrendale, PA, 2004, p 15-25
2. J. Sato, T. Ohmori, I. Ohnuma, R. Kainuma, and K. Ishida, Cobalt-Base High-Temperature Alloys, *Science*, 2006, **312**, p 90-91
3. J.O. Andersson and J. Agren, Models for Numerical Treatment of Multicomponent Diffusion in Simple Phases, *J. Appl. Phys.*, 1992, **72**(4), p 1350-1355
4. B. Jonsson, Ferromagnetic Ordering and Diffusion of Carbon and Nitrogen in bcc Cr-Fe-Ni Alloys, *Z. Metallkd.*, **85**(7), p 498-501
5. L. Hoglund and J. Agren, Analysis of the Kirkendall Effect, Marker Migration and Pore Formation, *Acta Mater.*, 2000, **49**(8), p 1311-1317
6. H. Strandlund and H. Larsson, Prediction of Kirkendall Shift and Porosity in Binary and Ternary Diffusion Couples, *Acta Mater.*, 2004, **52**(15), p 4695-4703
7. J.-O.Andersson, L. Höglund, B. Jönsson, and J. Ågren, Computer Simulation of Multicomponent Diffusional Transformations in Steel, *Fundamentals and Applications of Ternary Diffusion*, G.R. Purdy, Ed., Pergamon Press, New York, NY, 1990, p 153-163
8. J.O. Andersson, T. Helander, L. Höglund, P.F. Shi, and B. Sundman, THERMO-CALC & DICTRA, Computational Tools for Materials Science, *CALPHAD*, 2002, **26**(2), p 273-312

9. C.E. Campbell, W.J. Boettinger, and U.R. Kattner, Development of a Diffusion Mobility Database for Ni-Base Superalloys, *Acta Mater.*, 2002, **50**(4), p 775-792
10. J.Z. Zhu, L.-Q. Chen, J. Shen, and V. Tikare, Coarsening Kinetics from a Variable-Mobility Cahn-Hilliard Equation: Application of a Semi-implicit Fourier Spectral Method, *Phys. Rev. E*, 1999, **60**(4), p 3564-3572
11. J.Z. Zhu, T. Wang, A.J. Ardell, S.H. Zhou, Z.-K. Liu, and L.-Q. Chen, Three-Dimensional Phase-Field Simulations of Coarsening Kinetics of γ' Particles in Binary Ni-Al Alloys, *Acta Mater.*, 2004, **52**(9), p 2837-2845
12. Y.-W. Cui, K. Oikawa, R. Kainuma, and K. Ishida, Study of Diffusion Mobility of Al-Zn Solid Solution, *J. Phase Equilib. Diff.*, 2006, **27**(4), p 333-342
13. Y.-W. Cui, M. Jiang, I. Ohnuma, K. Oikawa, R. Kainuma, and K. Ishida, Computational Study of Atomic Mobility for fcc Phase of Co-Fe and Co-Ni Binaries, *J. Phase Equil. Diff.*, 2008, **29**(1), p 2-10
14. A.F. Guillermet, Assessing the Thermodynamics of the Fe-Co-Ni System Using a CALPHAD Predictive Technique, *CALPHAD*, 1989, **13**(1), p 1-22
15. J.P. Sabatier and A. Vignes, Study of Diffusion Phenomena in Ternary Fe-Ni-Co System, *Mem. Sci. Rev. Met.*, 1967, **64**(3), p 225-240
16. A. Vignes and J.P. Sabatier, Ternary Diffusion in Fe-Ni-Co Alloys, *Trans. Met. Soc. AIME*, 1969, **245**(8), p 1795-1802
17. Y.E. Ugaste, A.A. Kodentsov, and F. van Loo, Investigation of the Interdiffusion and Kirkendall Effect in the Co-Ni-Fe System: I. Redistribution of Component Concentrations in the Diffusion Zone and Shift of Inert Markers, *Phys. Metal Metallogr.*, 2004, **97**(3), p 298-306
18. Y.E. Ugaste, A.A. Kodentsov, and F. van Loo, Investigation of the Interdiffusion and Kirkendall Effect in the Co-Ni-Fe System: II. Effective and Partial Coefficients of Interdiffusion, *Phys. Metals Metallogr.*, 2004, **97**(5), p 495-501
19. R. Filipek, M. Danielewski, and R. Bachorczyk, Interdiffusion Studies in Co-Fe-Ni Alloys, *Defect Diff. Forum*, 2005, **237-240**, p 408-413
20. J. Priimets, A. Ainsaar, and U. Ugaste, Calculating of Diffusion Paths in Ternary Systems using Effective Interdiffusion Coefficients of Components, *Defect Diff. Forum*, 2005, **237-240**, p 1264-1269
21. M.A. Dayananda and Y.H. Sohn, Average Effective Interdiffusion Coefficients and Their Applications for Isothermal Multicomponent Diffusion Couples, *Scr. Mater.*, 1996, **35**(6), p 683-688
22. M.A. Dayananda and Y.H. Sohn, A New Analysis for the Determination of Ternary Interdiffusion Coefficients from a Single Diffusion Couple, *Metall. Mater. Trans.*, 1999, **30A**(3), p 535-543
23. J.S. Kirkaldy, Diffusion in Multicomponent Metallic Systems, *Can. J. Phys.*, 1957, **35**(4), p 435-440
24. M.A. Dayananda, Diffusion in Multicomponent Alloys: Challenges and Problems, *Defect Diff. Forum*, 1992, **83**, p 73-86
25. F.N. Fritsch and R.E. Carlson, Monotone Piecewise Cubic Interpolation, *SIAM J. Numer. Anal.*, 1980, **17**(2), p 238-246
26. W.H. Press, S.A. Teukolsky, W.T. Vetterling, and B.P. Flannery, *Numerical Recipes in C*. Cambridge University Press, Cambridge, UK, 1992, p 173-176
27. J.A. Nesbitt and R.W. Heckel, Interdiffusion in Ni-rich, Ni-Cr-Al Alloys at 1100 °C and 1200 °C-2: Diffusion Coefficients and Predicted Concentration Profiles, *Metall. Trans.*, 1987, **18A**(12), p 2075-2086
28. K. Wu, J.E. Morral, and Y. Wang, Movement of Kirkendall Markers, Second Phase Particles and the Type 0 Boundary in Two-Phase Diffusion Couple Simulations, *Acta Mater.*, 2004, **52**(7), p 1917-1925
29. M.J.H. van Dal, A.M. Gusak, C. Cserhati, A.A. Kodentsov, and F.J.J. van Loo, Microstructural Stability of the Kirkendall Plane in Solid-State Diffusion, *Phys. Rev. Lett.*, 2001, **86**(15), p 3352-3355
30. M.J.H. van Dal, A.M. Gusak, C. Cserhati, A.A. Kodentsov, and F.J.J. van Loo, Spatio-Temporal Instabilities of the Kirkendall Marker Planes during Interdiffusion in β'-AuZn, *Philos. Mag. A*, 2002, **82**(5), p 943-954
31. J.S. Kirkaldy, D. Weichert, and Zia-Ul-Haq, Diffusion in Multicomponent Metallic Systems-4-Some Thermodynamic Properties of D Matrix and Corresponding Solutions of Diffusion Equations, *Can. J. Phys*. 1963, **41**(12), p 2166-2173
32. H. Okamoto and T.B. Massalski, Thermodynamically Improbable Phase Diagrams, *J. Phase Equilib.*, 1991, **12**(2), p 148-168
33. A. Borgenstam, A. Engstrom, L. Hoglund, and J. Agren, DICTRA, a Tool for Simulation of Diffusional Transformations in Alloys, *J. Phase Equilib. Diff.*, 2000, **21**(3), p 269-280
34. M. Badia and A. Vignes, Iron, Nickel and Cobalt Diffusion in Transition Metals of Iron Group, *Acta Met.*, 1969, **17**(2), p 177-187, in French